

Effect of Lanthanum Doping on the Electrical Performance of Spray Coated ZnO Thin Film Transistor

Ravindra Naik Bukke, Narendra Naik Mude, Jewel Kumer Saha, Youngoo Kim, and Jin Jang

Advanced Display Research Center, Kyung Hee University, Dongdaemoon-ku, Seoul 02447, South Korea

Keywords: Lanthanum, solution-process, spray pyrolysis, thin-film transistor, ZnO

ABSTRACT

We studied the effect of lanthanum incorporation on the electrical properties of ZnO TFT fabricated by spray pyrolysis. The turn-on voltage (V_{ON}) shifts towards 0 V by La doping. Also, Subthreshold swing (SS) decreases significantly from 387 to 251 mV/dec, by incorporation of lanthanum in ZnO.

1. INTRODUCTION

Nowadays, the increasing attention towards metal oxide thin-film transistors (TFTs) to replace amorphous-Si (a-Si) or polycrystalline-Si (Poly-Si) based TFTs. The wide band-gap of zinc oxide (ZnO) with the wurtzite structure could be used as a channel layer in TFTs for display application.¹ The ZnO oxide TFTs can be manufactured via vacuum process² or solution process³⁻⁶. The spray coating⁷⁻⁸ and spin coating⁶ are common methods for the solution-processed oxide TFTs. Zn-based oxide semiconductors such as aluminum-doped zinc oxide (AlZnO), indium doped zinc oxide (InZnO), gallium Indium co-doped zinc oxide (GaInZnO), gallium Indium co-doped zinc oxide (HfInZnO), and lanthanum Indium zinc oxide (LaInZnO) have been reported. Doped metal carrier suppressors such as Al, Ga, Hf, Mg, Y, and Zr can improve the electrical performance of oxide TFTs. Also, the low standard electrode potential of the metal ion can reduce the oxygen vacancies concentration due to the strong bonding tendency with oxygen. In this work, we studied the effect of lanthanum doping on the electrical performance of ZnO TFT.

2. EXPERIMENT

2.1 Precursor Solution synthesis

The zirconium oxide (ZrO_x) precursor solution with a molar concentration of 0.2 M was prepared by dissolving zirconium chloride hydrate ($ZrOCl_2 \cdot xH_2O$) into the solvent mixture of acetonitrile (35%) and ethylene glycol (65%). The synthesis of ZrO_x solution is reported elsewhere.⁶ Lanthanum doped zinc oxide (LaZnO)

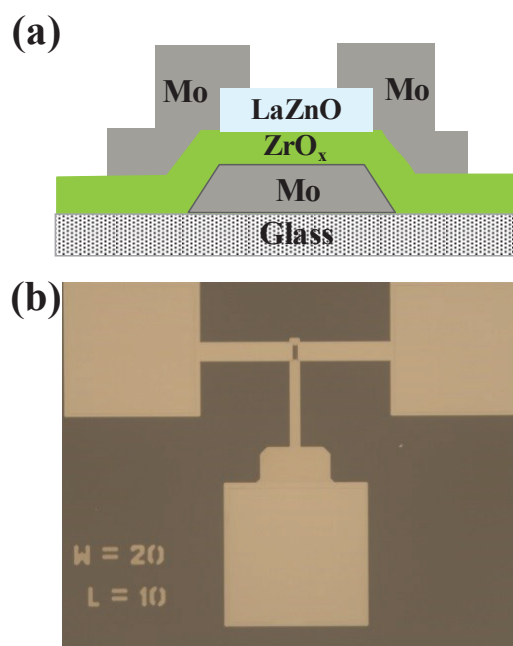


Fig. 1 (a) Schematic diagram for the cross-sectional image of the bottom gate - top contact (BG-TC) LaZnO TFT. (b) Optical photograph of fabricated LaZnO TFT, the extended part of Fig. 1(b) shows a clear active island region with a channel length and width of 10 and 20 μm .

solution was prepared by dissolving lanthanum nitrate hexahydrate, and zinc acetate dihydrate, into 2-methoxyethanol. All the precursor solutions were made in an N₂ environment and stirred 2 h to get a transparent solution. All these solutions were filtered using a 0.45 μm PTFE filter before spin or spray coating.

2.2 Device Fabrication

Figure 1(a) shows ZnO TFT with a bottom gate top contact (BG-TC) structure. Gate insulator (ZrO_x) was deposited by spin coating on molybdenum (Mo) gate electrode; then the sample was annealed at 300 °C for 2 h in a furnace under atmospheric condition. The ZnO semiconductor was deposited by spray pyrolysis at the

substrate temperature of 350 °C. After active island and via hole pattern, Mo was deposited by sputtering and patterned as source/drain electrodes. Fig. 1(b) shows the optical photograph of fabricated bottom gate top contact structured LaZnO TFT with channel length and width of 20 and 10 μm, respectively. The extended part of Fig. 1(b) shows a clear active island region. Current-voltage characteristics were measured with a semiconductor parameter analyzer Agilent 4156C. The transfer curve measured at the drain voltage (V_{DS}) of 0.1 V, by sweeping the gate voltage (V_{GS}) from -5 to +5 V. The hysteresis voltage (V_H) is measured at $I_{DS} = 10^{-11}$ A. The measurement performed under dark condition.

2.3 Measurements

The TFT characteristics were measured with an Agilent 4156C semiconductor parameter analyzer. The saturation mobility was obtained using the following equation.

$$I_D = \frac{WC_i}{2L} \mu (V_{GS} - V_{TH})^2 \dots\dots\dots (1)$$

Where I_D , C_i , V_{GS} , V_{TH} , W , and L are the drain current, the capacitance of the gate dielectric per unit area, gate to source voltage, threshold voltage, the channel width, and length, respectively. The subthreshold swing (SS) was calculated as the minimum value of the inverse slope of the $\log_{10}(I_D)$ versus V_G :

$$S.S = \frac{dV_g}{d(\log_{10} I_{DS})} \dots\dots\dots (2)$$

3. RESULTS AND DISCUSSION

Figure. 2 (a) shows transfer characteristics of ZnO TFTs without and with lanthanum doping, respectively. The electrical properties of the ZnO TFTs without lanthanum exhibits saturation mobility (μ_{sat}) of $9.64 \text{ cm}^2\text{V}^{-1}\text{s}^{-1}$, turn-on voltage (V_{ON}) of -1.95 V, subthreshold swing (SS) of 387 mV/dec, and hysteresis voltage (V_H) of 0.21 V. The electrical properties of the ZnO TFTs without lanthanum exhibits saturation mobility (μ_{sat}) of $4.94 \text{ cm}^2\text{V}^{-1}\text{s}^{-1}$, turn-on voltage (V_{ON}) of -0.30 V, subthreshold swing (SS) of 251 mV/dec, and hysteresis voltage (V_H) of ~0.05 V. The hysteresis voltage is measured at $I_{DS} = 10^{-11}$ A. The improvements in threshold swing and hysteresis are due to less interfacial traps at the LaZnO/ ZrO_x interface.

Table.1 Electrical properties of ZnO TFTs without and with La doping.

Channel Layer	μ_{sat} ($\text{cm}^2\text{V}^{-1}\text{s}^{-1}$)	V_{ON} (V)	SS (mV/dec)	Hysteresis (V_H)
ZnO	9.64	-1.95	387	0.21
LaZnO	4.94	-0.30	251	0.05

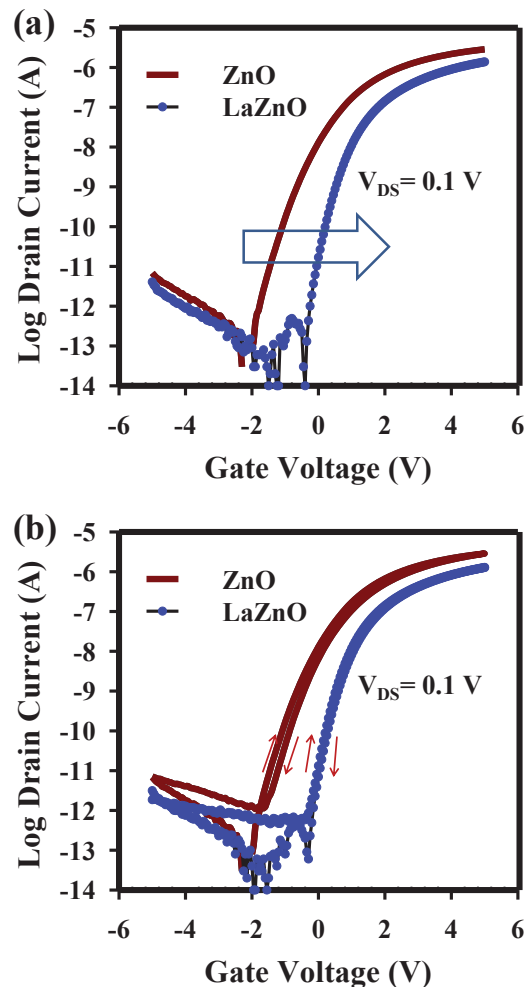


Fig. 2 (a) Transfer and (b) hysteresis curves of ZnO and LaZnO TFTs, respectively. The transfer curve measured at the drain voltage (V_{DS}) of 0.1 V, by sweeping the gate voltage (V_{GS}) from -5 to +5 V. The hysteresis voltage (V_H) is measured at $I_{DS} = 10^{-11}$ A by forward sweep of the V_{GS} from -5 to +5 V and reverse sweep from +5 to -5 V.

Fig. 3(a) and 3(b) shows the output characteristics of ZnO TFTs without and with lanthanum doping, respectively. The drain current in the saturation region of ZnO TFTs without and with lanthanum doping are 53 and 21.5 μA respectively. The output curves show clear pinch-off and saturation behavior, which indicates good ohmic contact between source/drain and the channel region. The electrical properties of ZnO TFT without and with lanthanum doping are summarized in Table 1.

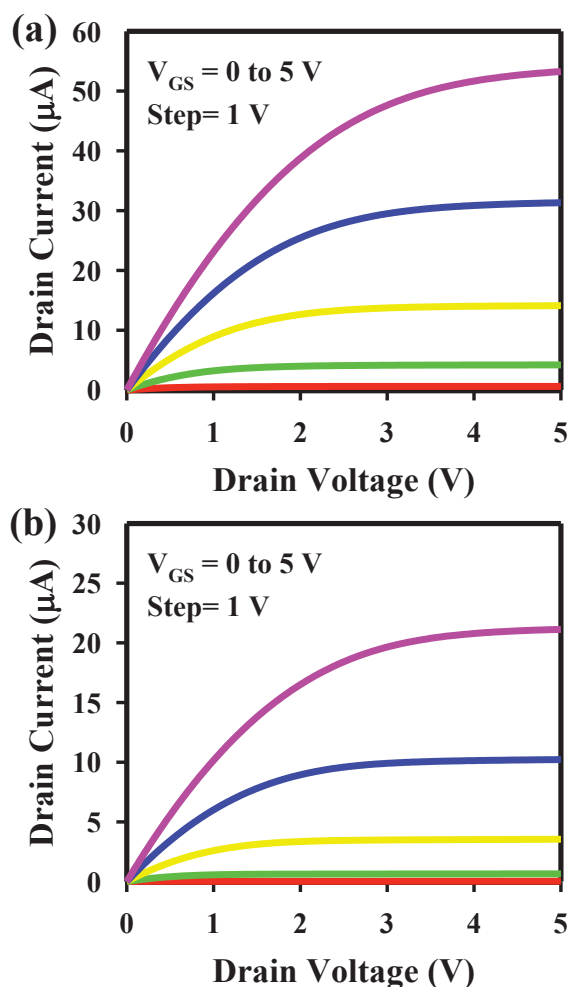


Fig. 3 Output curves of ZnO TFTs (a) without and (b) with lanthanum doping, respectively. V_{GS} sweeping from 0 to 5 V with a step of 1 V.

4. CONCLUSION

We studied the effect of lanthanum incorporation on the electrical properties of ZnO TFT fabricated by spray pyrolysis. The saturation mobility (μ_{sat}) increases from 9.64 to 4.94 $\text{cm}^2\text{V}^{-1}\text{s}^{-1}$, subthreshold swing (SS) decreased from 387 to 251 mV/dec, a decrease of hysteresis voltage from 0.21 to 0.05 V, and turn-on voltage (V_{ON}) decreased significantly from -1.95 to -0.3 V, by incorporation of lanthanum in ZnO. Therefore, these results suggest that lanthanum doping into ZnO can be a promising technique for fabricating high-performance oxide TFT.

Acknowledgment

The research was supported by the Korea Evaluation institute of Industrial Technology(KEIT) Development of

Core Technologies (Grant Number: 10070201) for Transportation Systems such as Green Car program funded by the Ministry of Trade, Industry and Energy(MOTIE).

References

- [1] L. Zhang, J. Li, X. Zhang, X. Jiang, and Z. Zhang, *Appl. Phys. Lett.*, 95, (2009), 072112.
- [2] M. Mativenga, D. Geng, B. Kim, and J. Jang, *Appl. Mater. Interf.* 7 (2015) 1578.
- [3] C. Avis and J. Jang: *J. Mater. Chem.* 21, (2011) 10649.
- [4] R. N. Bukke, C. Avis and J. Jang, *IEEE Electron Device Lett.* 01 (2016) 0093.R1
- [5] C. Avis, H. R. Hwang, and J. Jang, *Appl. Mater. Interf.* 6 (2014) 10941.
- [6] R. N. Bukke, M. N. Naik, C. Avis, and J. Jang, *IEEE Electron Device Lett.* 39, (2018), 371.
- [7] G. Adamopoulos, S. Thomas, P. H. Wöbkenberg, D. DC. Bradley, M. A. McLachlan, and T. D. Anthopoulos, *Adv. Mater.*, 23 (2011), 1894.
- [8] X. Yu, J. Smith, N. Zhou, L. Zeng, P. Guo, Y. Xia, A. Alvarez, S. Aghion, H. Lin, J. Yu, R. P. Chang, M. J. Bedzyk, R. Ferragut, T. J. Marks, A. Facchetti, *Proc. Natl. Acad. Sci. U. S. A.* 112 (2015), 3217.